Am J Transl Res 2016;8(5):2033-2046
www.ajtr.org /ISSN:1943-8141/AJTR0029529

Original Article

Isoflurane attenuates lipopolysaccharide-induced acute lung injury by inhibiting ROS-mediated NLRP3 inflammasome activation

Ning Yin, Zhendan Peng, Bin Li, Jiangyan Xia, Zhen Wang, Jing Yuan, Lei Fang, Xinjiang Lu

Department of Anesthesiology, Zhongda Hospital, School of Medicine, Southeast University, Nanjing 210009, Jiangsu, China

Received March 31, 2016; Accepted April 22, 2016; Epub May 15, 2016; Published May 30, 2016

Abstract: Nucleotide-binding domains and leucine-rich repeat (NLR) pyrin domains containing 3 (NLRP3) inflammasome are highly involved in the pathogenesis of acute lung injury (ALI) wherein alveolar macrophages (AMs) play a crucial role. Isoflurane (ISO) has been shown to attenuate ALI. However, the inhibitory effects of ISO on NLRP3 activation in lipopolysaccharide (LPS)-induced ALI remain unknown. Here, we showed that 1.4% ISO post-treatment reduced LPS-induced body weight loss, pulmonary histopathological injury, edema, and vascular permeability in rats. ISO attenuated LPS-triggered inflammation, as evidenced by reductions in the number of total cells, neutrophils, and macrophages, and the release of IL-1β and IL-18 in the bronchoalveolar lavage fluid. ISO treatment decreased the myeloperoxidase activity, F4/80-positive cells, and the mRNA expression of IL-1β and IL-18 in the lung tissues of LPS-treated rats. Mechanistically, ISO reduced NLRP3 activation and caspase-1 activity in a reactive oxygen species (ROS)-dependent manner. An in vitro study that ISO inhibited LPS-induced AM activation partly confirmed in vivo findings. Overall, these results indicate that ISO post-conditioning alleviated LPS-induced ALI possibly by inhibiting ROS-mediated NLRP3 inflammasome activation.

Keywords: Acute lung injury, lipopolysaccharide, isoflurane, nucleotide-binding domain and leucine-rich repeat pyrin domain containing 3, reactive oxygen species

Introduction

Acute lung injury (ALI) and its more severe form, acute respiratory distress syndrome (ARDS), are common and devastating clinical disorders with high morbidity and mortality [1]. ALI is characterized by intense inflammation with neutrophil accumulation, interstitial edema, disruption of endothelial and epithelial integrity, and leakage of protein into the alveolar space. These symptoms lead to pulmonary edema, intrapulmonary hemorrhage, and severely impaired pulmonary gas exchange [2]. Despite several decades of striving for ALI therapy, its mortality rate has not improved significantly. Thus, probing the molecular mechanisms of ALI and exploring novel therapeutic regimens are urgent necessities.

The nucleotide-binding domains and leucine-rich repeat (NLR) pyrin domains containing 3 (NLRP3) inflammasome is a multiprotein complex composed of NLRP3, an apoptosis-associated speck-like protein containing a caspase activation and recruitment domain (ASC), and caspase-1 [3]. NLRP3 is the best-characterized member of NLRs involved in the innate and adaptive immune systems, which can be activated by exogenous and endogenous stimulating factors, such as bacteria, viruses, fungi, and components of dying cells [3, 4]. Signals from these various stimuli converge on a pathway that involves ionic balance, lysosome dysregulation, and mitochondrial damage, leading to the release of cathepsins and production of reactive oxygen species (ROS) [5]. ROS has been implicated as a positive regulator of NLRP3 inflammasome activation [6]. Upon activation, caspase-1 can cleave the proforms of interleukin (IL)-1β and IL-18 into their mature and active forms, which is followed by pyroptosis [5]. IL-1β is one of the most potent inflammation-initiating cytokines observed in ALI patients; it also induces the production of other

cytokines [7]. IL-18 functions as a pro-inflammatory cytokine in ALI, serving as both an autocrine activator and a facilitator of other inflammatory mediators [8]. NLRP3 inflammasome activation and IL-1β and IL-18 production are simultaneously augmented in the lungs of ALI mice with lipopolysaccharide (LPS) challenge [9-11]. Therefore, inactivating NLRP3 inflammasome may be an effective therapeutic technique for ALI.

Alveolar macrophages (AMs) residing in the alveolar space account for 90% of the cells in the bronchoalveolar lavage fluid (BALF) [12]. AMs are the primary source of cytokines in lungs and play an important role in the pathogenesis of ALI, initiating inflammatory responses and promoting neutrophil infiltration and tissue damage [13]. AMs from ARDS patients secrete much higher levels of IL-1β [14], and AM depletion results in significantly diminished IL-1β secretion and injury in animal models of ALI [15, 16]. NLRP3 inflammasome activation in AMs increases caspase-1 activity and IL-1β production, both of which aggravate lung injury [17]. Thus, the inhibition of NLRP3 inflammasome activation in AMs possibly contributes to the attenuation of inflammation-related lung damage.

Isoflurane (ISO) exerts anti-inflammatory and anti-oxidative effects in multiple organs, including the lungs [18-21]. Inhalation of ISO elicits protective effects during zymosan-, LPS-, or ischemia-reperfusion-induced lung injury [21-24]. Previous studies have revealed that ISO prevents LPS-induced lung damage by reducing cytokine release from alveolar macrophages, neutrophil recruitment and microvascular protein leakage [25-28]. However, the protective effects of ISO and underlying mechanisms in LPS-induced ALI remain unclear.

In this study, we found that 1.4% ISO post-treatment significantly improved the body weight loss and attenuated the pulmonary histopathological damage, edema and vascular leakage in LPS-induced ALI animals. ISO reduced the number of total cells, neutrophils, and macrophages, and the release of IL-1β and IL-18 in the BALF of LPS-treated rats. ISO decreased myeloperoxidase (MPO) activity, F4/80-positive cells, and mRNA expression of IL-1β and IL-18 in the lungs of LPS-challenged rats. ISO also inhibited NLRP3 inflammasome activation and caspase-1 activity partly by scavenging ROS. In vitro studies of LPS-treated AMs were consistent with in vivo findings. Together, ISO post-treatment attenuated LPS-induced ALI partially by inhibiting ROS-mediated NLRP3 inflammasome activation.

Materials and methods

Animals

Male Sprague-Dawley rats (6 weeks, 200-250 g) were provided by the Laboratory Animal Center of Southeast University (Nanjing, Jiangsu, China) and housed in pathogen-free conditions with a 12 h/12 h light/dark cycle at 22-24°C and free access to food and water. The experimental protocols were approved by the Institutional Animal Care Committee of Southeast University and conducted in accordance with the National Institutes of Health Guidelines for the Care and Use of Laboratory Animals.

LPS-induced ALI and ISO treatment

The LPS-induced ALI model was established as previously described [23]. Briefly, rats were injected intraperitoneally (i.p.) with LPS (*Escherichia coli* 055:B5; Sigma-Aldrich, St. Louis, MO, USA) at a dose of 30 mg/kg body weight. Sham controls were injected i.p. with the same volume of aseptic saline. At 1 h after LPS or saline administration, the rats were treated with ISO as previous report [23]. The animals were placed in a rodent ventilator (ALC-V8, Shanghai AlcottBiotech Co., Shanghai, China), and the ISO concentration (1.4%) was maintained for 1 h and monitored by a gas-specific analyzer (Capnomac Ultima; Datex, Helsinki, Finland) during treatment. Rats without ISO treatment were exposed to room air (RA) in the chamber as a vehicle control. In summary, the rats were divided into four groups: the sham + RA group, the sham + ISO group, the LPS + RA group, and the LPS + ISO group. In experiments involving ROS scavengers, the rats were injected intravenously (i.v.) with 150 mg/kg *N*-acetylcysteine (NAC; Sigma) 30 min before LPS injection. All of the rats were euthanized under anesthesia at 12 h after LPS exposure.

Isolation of AMs

AMs were isolated from the BALF as previously described [29]. Briefly, healthy rats were eutha-

nized by sodium pentobarbital. Lungs and the trachea were then excised completely, washed in Hank's balanced salt solution (HBSS), and lavaged over 10 times with light massaging by slowly instilling and withdrawing 1 mL of warm (37°C) Ca^{2+}/Mg^{2+}-free HBSS (pH 7.4) containing ethylene diamine tetraacetic acid (0.6 mM). BALF was collected and centrifuged at 400 × *g* at 4°C for 10 min. The cells were then incubated in 100 mm sterilized polystyrene Petri dishes at 37°C for 2 h. Cells adhered to the bottom of the dish were harvested and replated for further experiments. Phycoerythrin-conjugated anti-CD11b and fluorescein isothiocyanate- conjugatedanti-F4/80 (both obtained from eBioscience, San Diego, CA, USA) were used to confirm the > 95% purity of AMs by flow cytometric analysis. Viability was determined to be > 98% by trypan blue (Sigma) exclusion.

AMs culture and treatment

AMs were cultured at a density of 1×10^5 cells/cm^2 in collagen IV-coated dishes in DMEM (Gibco, BRL, Grand Island, NY, USA) containing 10% fetal calf serum (FBS; Gibco) without antibiotics and incubated at 37°C in an atmosphere of 5% CO_2. Confluent monolayers formed on the culture dishes or BioFlex plates with elastomer membranes within 24-48 h. AM monolayers were serum-deprived for 2 h prior to the experiments. AMs were treated with LPS (100 ng/mL) or culture medium (CM) for 30 min and then exposed to RA or ISO for 30 min in a metabolic chamber (Columbus Instruments, Columbus, OH, USA). During ISO exposure, the concentration of ISO (1.4%) was verified by Datex Capnomac exhaust gas (SOMA Technology Inc., Cheshire, CT, USA). The cells were cultured continuously for the indicated times. Four treatment groups were established, namely, the sham + RA group, the sham + ISO group, the LPS + RA group, and the LPS + ISO group. To investigate the inhibitory effects of NAC, AMs were pretreated with or without 1 mM NAC for 30 min, washed, and treated with LPS or new CM for the indicated time periods.

Sample collection

At 12 h after LPS injection, the rats were anesthetized using sodium pentobarbital. Blood samples were taken from the ventral aorta and centrifuged at 1500 × *g* for 10 min; the serum was collected and stored at -20°C before use. The lower lobe of the right lung was ligated prior to bronchoalveolar lavage (BAL) and harvested for the determination of MPO and caspase-1 activities, and quantitative real-time PCR (qPCR), Western blot, and histopathological analyses. BAL was performed as previously described [30]. Briefly, after anesthetization, the trachea was exposed and cannulated with a 22-G intravenous cannula. Phosphate-buffered saline (PBS; 0.8 mL) was injected and withdrawn for the first lavage. The lavage procedure was performed thrice. BALF samples were centrifuged at 1000 × *g* for 8 min at 4°C. The supernatants were harvested for cell counting, enzyme-linked immunosorbent assay (ELISA), and total protein analysis. Cell pellets were resuspended in PBS, and the number of cells was determined with a hemocytometer (Beckman Coulter, Inc.). Differential cell counts were enumerated on cytospin-prepared slides stained with Diff-Quick stain (Andwin Scientific, Schaumburg, IL, USA). Protein content was assessed by using a bicinchoninic acid protein assay kit (Thermo Fisher Scientific, Rockford, IL, USA) in accordance with the manufacturer's instructions. The ratio of BALF/serum protein concentration was used as the lung permeability index (LPI).

Histology and immunohistochemistry analysis

Lung samples were fixed with 4% paraformaldehyde for 48 h at room temperature, embedded in paraffin, and sectioned to 4 μm thicknesses. After deparaffinization and rehydration, the sections were stained with hematoxylin and eosin (HE; Sigma) for examination by light microscopy (Olympus, Tokyo, Japan). A scoring system to grade the degree of lung injury was used, based on predetermined criteria. The scores obtained through this system represent the average of scores given by two independent investigators tasked to read each HE-stained slide in a blinded manner. All points for each category were added and weighted according to their relative importance. The injury score was calculated according to the following formula: injury score = [(alveolar hemorrhage points/no. of fields) + 2 × (alveolar infiltrate points/no. of fields) + 3 × (fibrinpoints/no. of fields) + (alveolar septal congestion/no. of fields)]/total number of alveoli counted. Rabbit anti-rat F4/80 polyclonal antibody (Abcam, Cambridge, UK) was used to immunostain tissues. F4/80 protein was visualized using diaminobenzidine, and images were obtained using a light microscope (Olympus) with the QImaging software

(Surrey, BC, Canada). The number of $F4/80^+$ cells in the lung was counted in 20 consecutive high-power fields (hpf, × 40) and expressed as cells/hpf.

Lung wet/dry (W/D) weight ratio

Lung edema was estimated by the W/D weight ratio. Fresh lung was weighed, dried in an oven at 80°C for at least 24 h, and then weighed again after drying to calculate the W/D weight ratio.

Capillary protein leakage

Pulmonary capillary permeability was determined using the Evans blue dye extravasation technique. The animals received tail vein injections of Evans blue dye (30 mg/kg; Sigma) 30 min before sacrifice. Following the rats' death, PBS-perfused lungs were harvested. Evans blue content was measured at 620 nm using a spectrophotometer (Beckman, Fullerton, CA, USA), and Evans blue permeability was calculated and expressed as μg/g of lung.

Lung MPO activity

MPO activity, a marker of neutrophil infiltration in the lung, was determined using an MPO assay kit (Nanjing Jiancheng Bioengineering Institute, Nanjing, China) according to the manufacturer's protocol. Briefly, 100 mg of lung tissue was homogenized in extraction buffer. The samples were maintained at 37°C for 15 min, and enzymatic activity was subsequently measured using a spectrophotometer (Beckman) at 460 nm. MPO activity was expressed as U/mg lung.

ELISA

Levels of IL-1β and IL-18 in the BALF or cell supernatants were measured using ELISA kits (R&D Systems, Minneapolis, MN, USA) according to the manufacturer's protocols. A microplate reader (Molecular Devices, Sunnyvale, CA, USA) was used to measure optical density at 450 nm.

qPCR

Total RNA from lung tissues or cultured AMs was extracted using TRIzol reagent (Invitrogen, CA, USA). cDNA was generated using a Prime Script RT Reagent Kit (Takara, Otsu, Shiga, Japan). Real-time PCR was performed using SYBR Green Supermix (Bio-Rad, Hercules, CA, USA). Results were analyzed by the $2^{-\Delta\Delta Ct}$ method for relative quantitation and normalized to glyceraldehyde-3-phosphate dehydrogenase (GAPDH). The following primers were used: for NLRP3, 5'-CAGCG ATCAACAGGCGAGAC-3' (forward), and 5'-AGAGATATCCCAGCAAACCTATC CA-3' (reverse); for ASC, 5'-ACTCATTGCCAGG-GTCACAGAAGTG-3' (forward), and 5'-GCTTC-CTCATCTTGTCTTGGCTGGT-3' (reverse); for caspase-1, 5'-ACTCG TACACGTCTTGCCCTCA-3' (forward), and 5'-CTGGGCAGGCAGCAAATTC-3' (reverse); for IL-1β, 5'-CCCTGAACTCAACTGTGAAA-TAGCA-3' (forward), and 5'-CCCAAGTCAAGGG-CTTGGAA-3' (reverse); for IL-18 5'-GACTGGC-TGTGAC CCTATCTGTGA-3' (forward), and 5'-TT-GTGTCCTGGCACACGTTTC-3' (reverse); and for GAPDH, 5'-GAACATCATCCCTGCATCCA-3' (forward), and 5'-CCAGTGA GCTTCCCGTTCA-3' (reverse).

Measurement of ROS production

Levels of intracellular ROS were measured by the oxidative conversion of 2',7'-dichlorofluorescein diacetate (DCFH-DA) to the fluorescent compound dichlorofluorescin (DCF). In brief, lung homogenates or AMs were incubated with PBS containing 15 μM 2',7'-DCFH-DA (Nanjing Jiancheng Bioengineering Institute) for 30 min at 37°C to label intracellular ROS. The cells were then washed with PBS, and cellular fluorescence was determined using a microplate reader (Promega, Madison, WI, USA) at 490 and 520 nm.

Caspase-1 activity assay

Caspase-1 enzymatic activity was measured using a colorimetric assay kit (R&D system). Briefly, lung homogenates or cell supernatants were added to 50 μL of caspase-1 reaction buffer and 40 μM YVAD-pNA (Santa Cruz, CA, USA), a caspase-1 substrate, followed by incubation at 37°C for 2 h. Caspase-1 activity was measured at 405 nm using a microplate reader (Promega).

Western blot analysis

Proteins were extracted from lung tissues or cultured AMs with lysis buffer (Cell Signaling Technology, Beverly, MA, USA). Equal samples were separated by sodiumdodecyl sulfate polyacrylamide gel and electrophoretically trans-

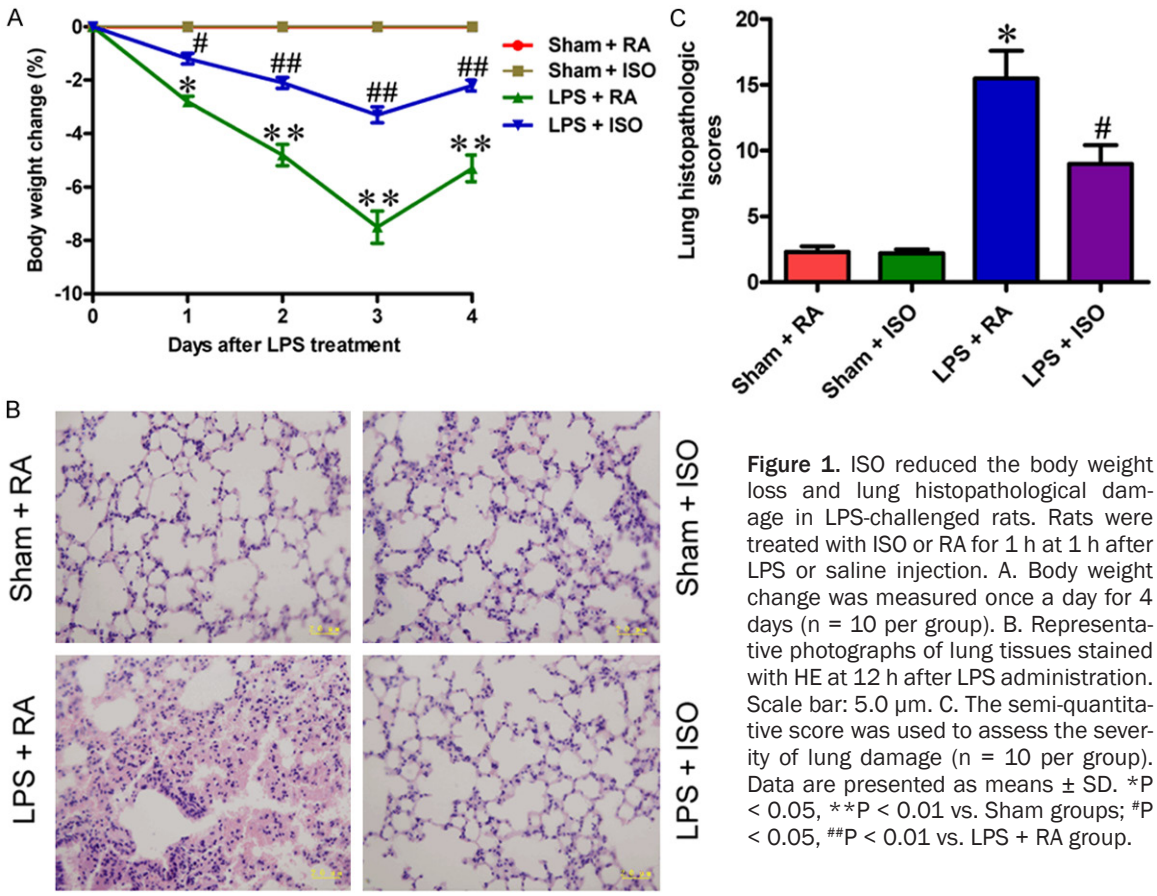

Figure 1. ISO reduced the body weight loss and lung histopathological damage in LPS-challenged rats. Rats were treated with ISO or RA for 1 h at 1 h after LPS or saline injection. A. Body weight change was measured once a day for 4 days (n = 10 per group). B. Representative photographs of lung tissues stained with HE at 12 h after LPS administration. Scale bar: 5.0 μm. C. The semi-quantitative score was used to assess the severity of lung damage (n = 10 per group). Data are presented as means ± SD. *P < 0.05, **P < 0.01 vs. Sham groups; #P < 0.05, ##P < 0.01 vs. LPS + RA group.

ferred to a nitrocellulose membrane (Millipore, Bedford, MA, USA). The membranes were blocked with 5% skim milk in Tris-buffered saline with Tween-20 for 1 h at room temperature. Blots were then incubated overnight with rabbit anti-rat polyclonal antibodies such as NLRP3, ASC, caspase1-p20 (all obtained from Adipogen, San Diego, CA, USA), and β-actin (Cell Signaling Technology) at 4°C. Horseradish peroxidase-conjugated anti-rabbit IgG (Cell Signaling Technology) was used as a secondary antibody. Signals were detected using an enhanced chemiluminescence kit (Cell Signaling Technology). The density of each protein band on the membrane is reported as the densitometric ratio between the protein of interest and β-actin.

Statistical analysis

All of the data, except for the histopathological scores, are presented as means ± standard deviation (SD). Histopathological scores were obtained using the nonparametric Kruskal-Wallis method followed by the Nemenyi multiple comparison test. Intergroup differences were determined using one-way analysis of variance followed by Tukey's test for multiple comparisons. Statistical analyses were accomplished by SPSS 16.0 (Chicago, IL, USA), and $P < 0.05$ was considered significant difference.

Results

ISO protects rats against LPS-induced body weight loss and histopathological damage

The body weight of the rats was significantly reduced after LPS administration (**Figure 1A**). However, ISO post-treatment attenuated the body weight loss induced by LPS stimulation (**Figure 1A**). The protective effects of ISO on LPS-induced lung injury were investigated by histological examination with HE staining. As shown in **Figure 1B**, LPS challenge caused severe lung injury characterized by pulmonary edema, hemorrhage, alveolar wall thickening, and intraalveolar exudation. LPS treatment also resulted in the infiltration of inflammatory cells into the lung interstitium and alveolar spaces. However, ISO post-conditioning attenuated the above histopathological changes. Evaluation of the pathological severity of lung

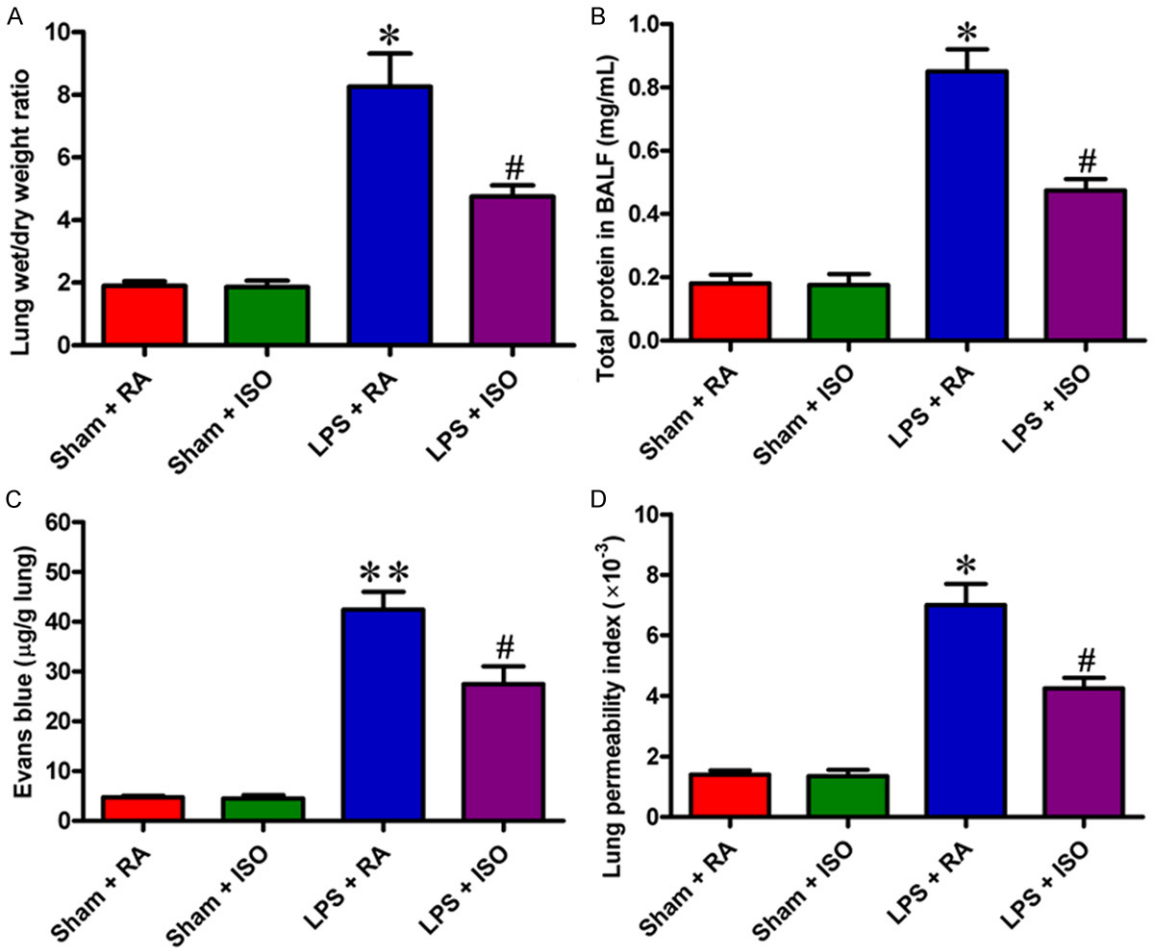

Figure 2. ISO improved LPS-induced lung edema and capillary permeability in rats. Rats were treated with ISO or RA for 1 h at 1 h after LPS or saline injection. Lung tissue, BALF, and blood samples were harvested to evaluate the hallmarks of lung injury at 12 h after LPS or saline challenge. (A) The W/D weight ratio of lung. (B) The protein leakage in the BALF. (C, D) The lung capillary permeability was evaluated by Evans blue extravasation (C) and LPI (D). Data are presented as means ± SD (n = 10 per group). *P < 0.05, **P < 0.01 vs. sham groups; #P < 0.05 vs. LPS + RA group.

injury through independent scoring four parameters showed a significant decrease in the histopathological score of the LPS + ISO group compared to that of the LPS + RA group (**Figure 1C**). These results suggest that ISO treatment significantly alleviated LPS-induced body weight loss and lung injury of rats.

ISO mitigates LPS-induced pulmonary edema and capillary permeability in rats

To evaluate the protective effects of ISO on LPS-induced lung injury further, lung W/D weight ratio, total protein in the BALF, and pulmonary capillary permeability were assessed. The lung W/D weight ratio, a well-known hallmark of lung edema, significantly increased in LPS-treated rats (**Figure 2A**). In terms of lung permeability and vascular leakage, total protein level in the BALF of LPS-challenged rats was very high (**Figure 2B**). Evans blue extravasation assay indicated that LPS induced a significant increase in Evans blue leakage into the lung (**Figure 2C**). Similar results were obtained for LPI, another good indicator of alveolar-capillary permeability (**Figure 2D**). ISO post-treatment markedly reduced the increases in lung W/D weight ratio, total protein in the BALF, Evans blue leakage, and LPI induced by LPS (**Figure 2A-D**). These data demonstrate that ISO treatment reduced lung edema and capillary leakage in LPS-treated rats.

ISO inhibits LPS-induced inflammatory response in rats

To investigate the effect of ISO on LPS-induced inflammatory response in lung, the number of

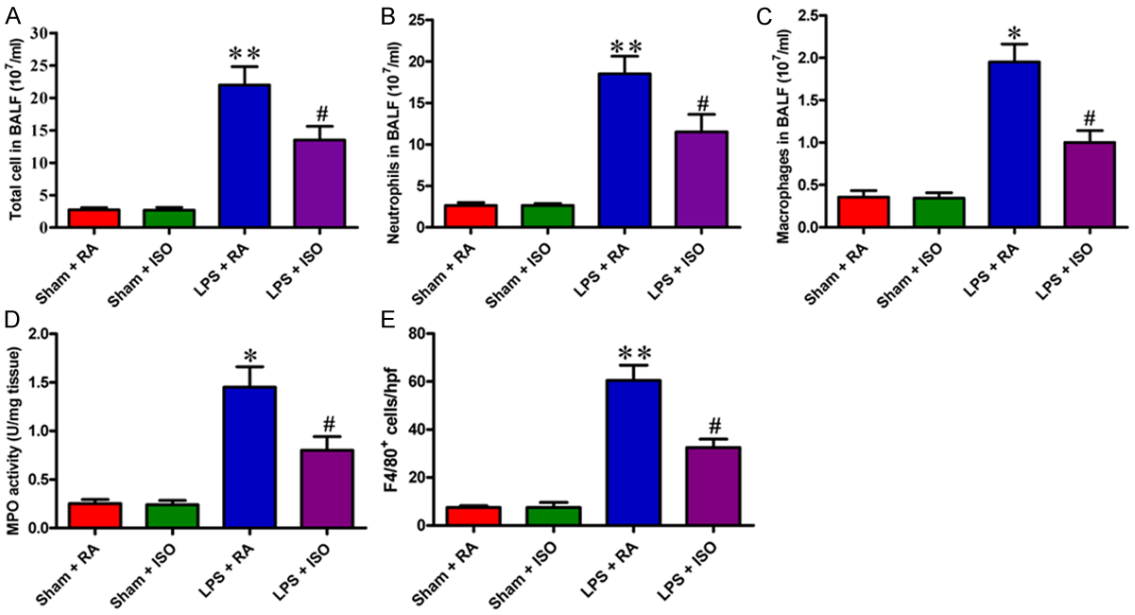

Figure 3. ISO reduced inflammatory cells of lung in LPS-stimulated rats. Rats were treated with ISO or RA for 1 h at 1 h after LPS or saline injection. Lung and BALF samples were collected at 12 h after LPS or saline administration. (A-C) The number of (A) total cells, (B) neutrophils, and (C) macrophages in the BALF were measured using a hemocytometer. (D) MPO activity in lung. (E) Immunohistochemistry staining of F4/80-positive macrophages in lung tissues. Results were scored semi-quantitatively by averaging the number of stained cells per field. Data are presented as means ± SD (n = 10 per group). *P < 0.05, **P < 0.01 vs. sham groups; #P < 0.05 vs. LPS + RA group.

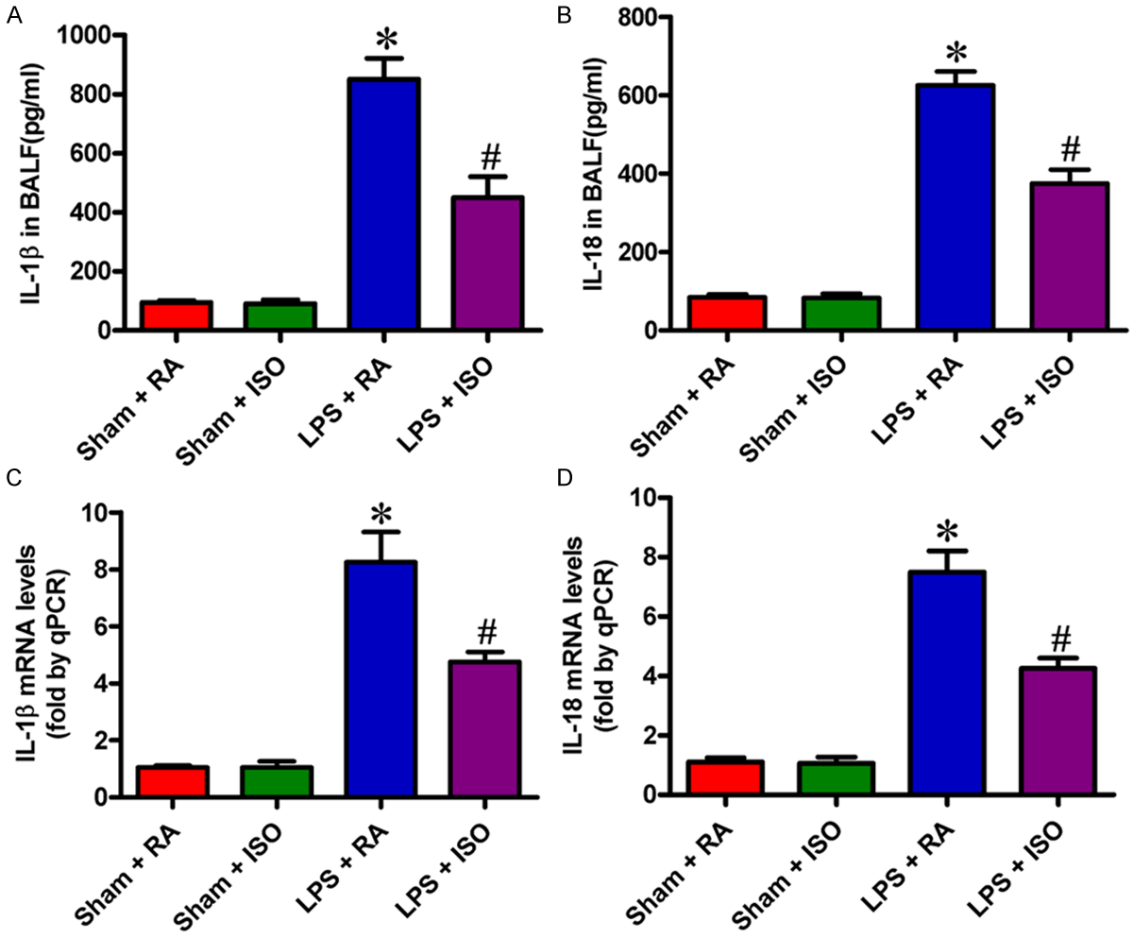

Figure 4. ISO reduced the levels of IL-1β and IL-18 in BALF and lung tissues of LPS-treated rats. Rats were treated with ISO or RA for 1 h at 1 h after LPS or saline injection. Lung tissue and BALF samples were collected at 12 h after LPS or saline administration. (A, B) The levels of IL-1β (A) and IL-18 (B) in the BALF were measured by ELISAs. (C, D) The mRNA expression of IL-1β (C) and IL-18 (D) in lung was analyzed by qPCR assay. GAPDH was used as the endogenous control. Data are presented as means ± SD (n = 10 per group). *P < 0.05 vs. sham groups; #P < 0.05 vs. LPS + RA group.

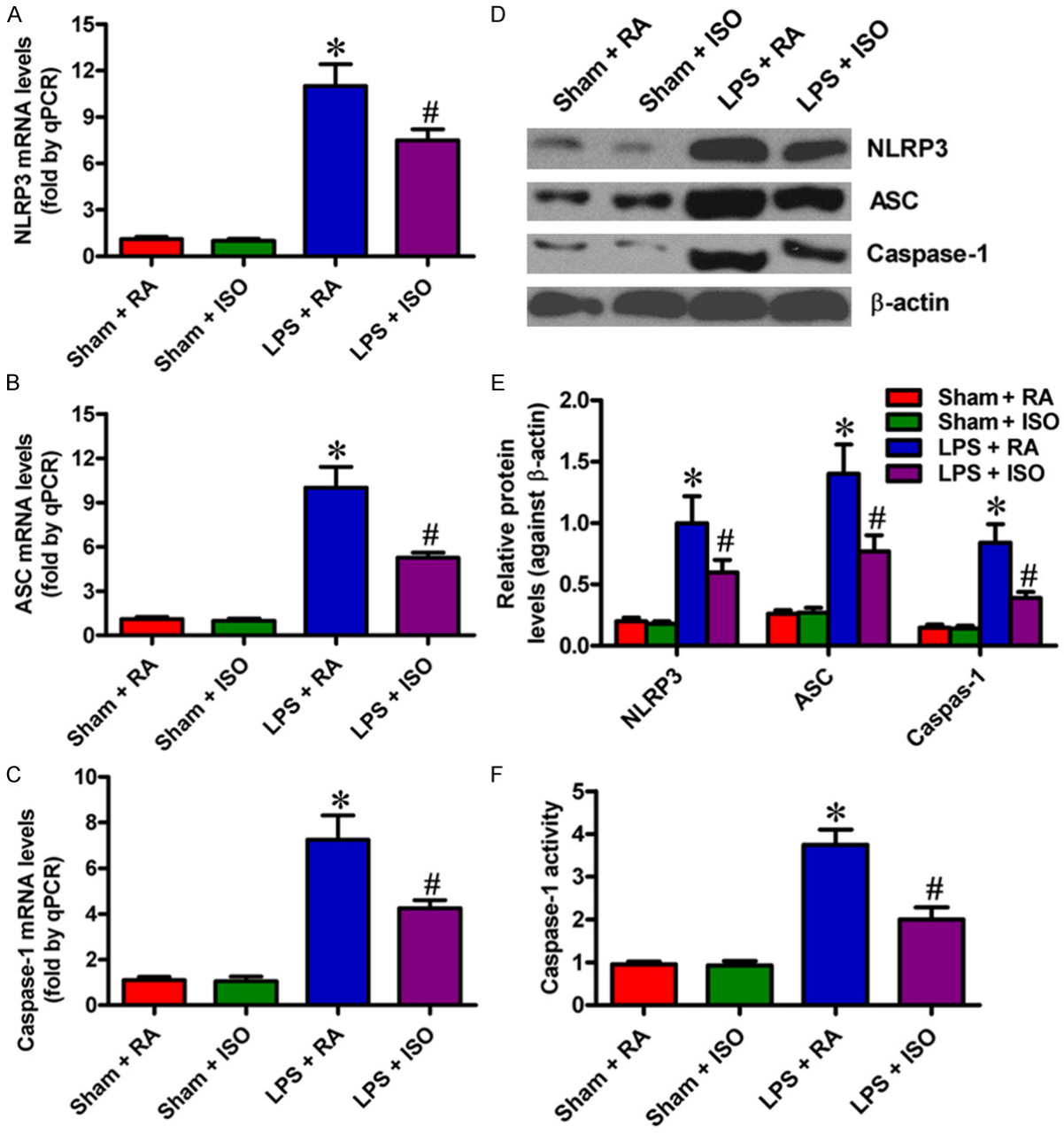

Figure 5. ISO inhibited LPS-induced NLRP3 inflammasome activation in the lung of rats. Rats were treated with ISO or RA for 1 h at 1 h after LPS or saline injection. Lung samples were collected at 12 h after LPS or saline administration. (A-C) qPCR assay was performed to determine the mRNA expression of NLRP3 (A), ASC (B), and caspase-1 (C) in lung tissues. GAPDH was used as the endogenous control. (D) Representative results of western blot for NLRP3, ASC, and caspase-1-p20 expression in lung tissues. β-actin was used as the endogenous control. (E) Relative expression of NLRP3, ASC, and caspase-1-p20 was normalized to that of β-actin. (F) Caspase-1 activity in lung tissues. Data are presented as means ± SD (n = 10 per group). *P < 0.05 vs. sham groups; #P < 0.05 vs. LPS + RA group.

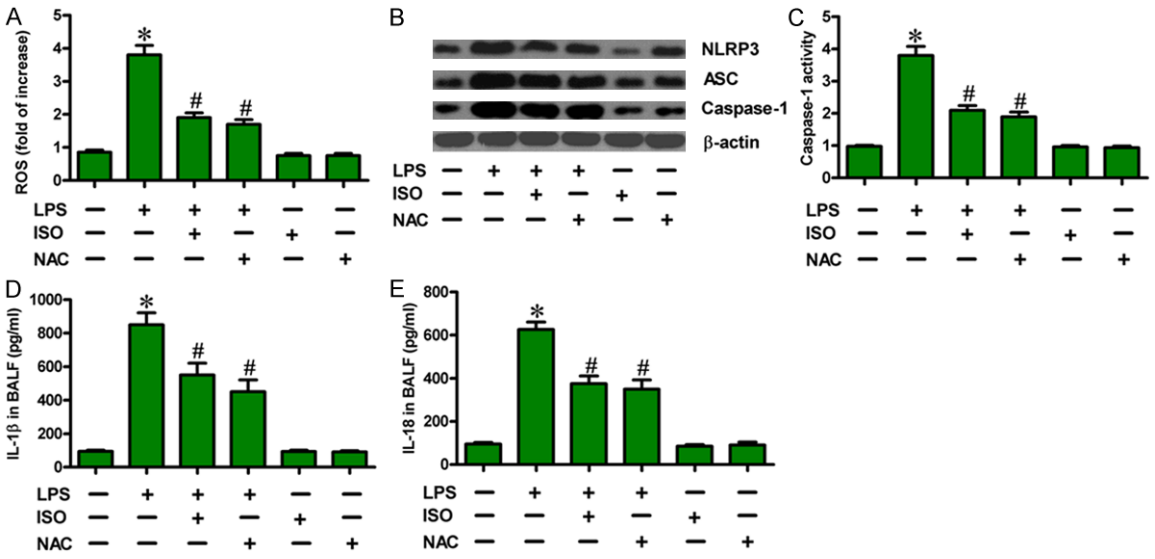

Figure 6. ISO-mediated inhibition of NLRP3 inflammasome activation was dependent on ROS in LPS-treated rats. Rats were treated with ISO/RA for 1 h at 1 h after LPS/saline injection or rats were injected with NAC at 30 min before LPS/saline treatment. Lung and BALF samples were collected at 12 h after LPS or saline administration. (A) ROS production in lung was assessed by DCFH-DA assay. (B) The expression of NLRP3, ASC, and caspase-1-p20 in lung was analyzed by western blot. β-actin was used as the endogenous control. (C) Caspase-1 activity in lung tissues. (D, E) ELISA was performed to determine the release of IL-1β (D) and IL-18 (E) in the BALF. Data are presented as means ± SD (n = 10 per group). *P < 0.05 vs. sham group; #P < 0.05 vs. LPS alone group.

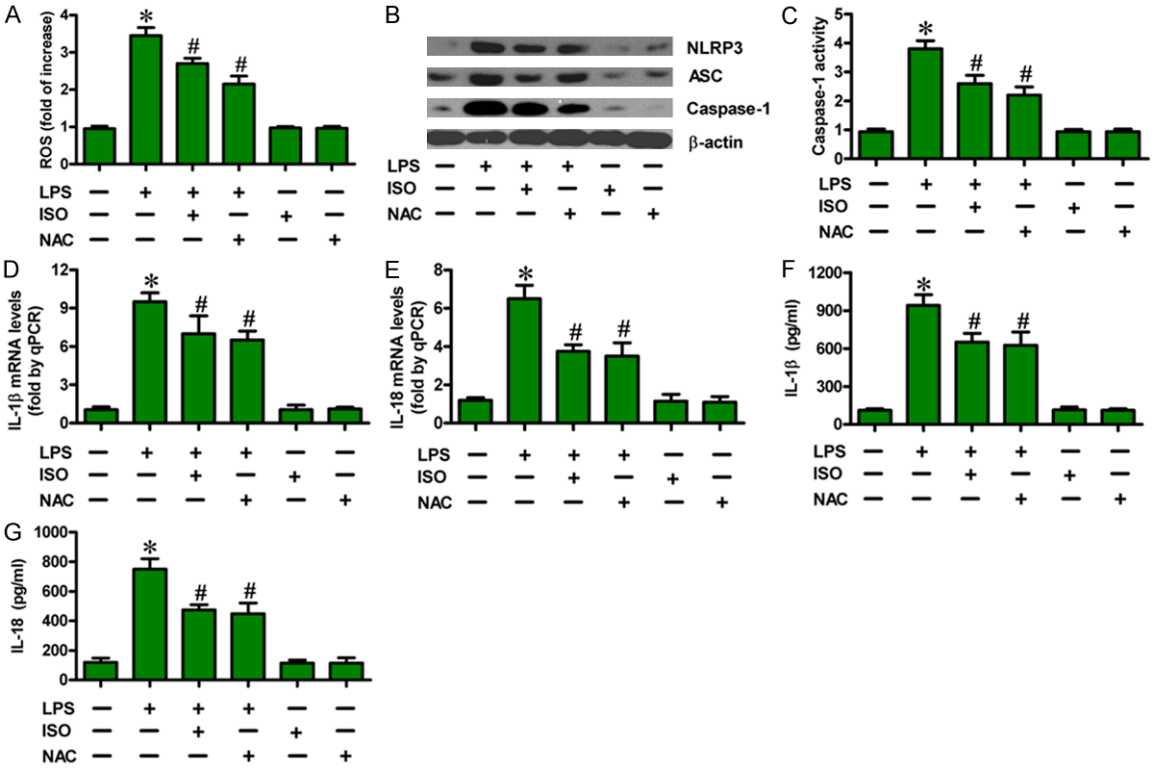

Figure 7. Inhibition of NLRP3 inflammasome activation by ISO was mediated by ROS in LPS-treated AMs in vitro. AMs were treated with ISO/RA for 30 min at 30 min after LPS/CM stimulation or AMs were pretreated with or without NAC at 30 min before LPS/CM stimulation. At 12 h after LPS/CM treatment, the cells and the supernatants were pooled for the subsequent experiments. (A) The levels of ROS in AMs. (B) Western blot analysis of NLRP3, ASC, and

caspase-1-p20 in AMs. β-actin was used as the endogenous control. (C) Caspase-1 activity in AMs. (D, E) The mRNA expression of IL-1β (D) and IL-18 (E) in AMs was measured by qPCR assay. GAPDH was used as the endogenous control. (F, G) The release of IL-1β (F) and IL-18 (G) in the supernatants was determined by ELISA. Data are presented as means ± SD. *P < 0.05 vs. sham group; #P < 0.05 vs. LPS alone group.

total cells, neutrophils, and macrophages in the BALF were measured using a hemocytometer. As shown in **Figure 3A-C**, LPS administration significantly increased the number of total cells, neutrophils, and macrophages in the BALF; ISO treatment attenuated these increases. MPO activity, which indicates the accumulation of neutrophils in the lung, showed a similar result (**Figure 3D**). Immunohistochemistry results showed a large number of F4/80-positive cells in LPS-induced injured lungs, which was significantly reduced by ISO treatment (**Figure 3E**). These results indicate that ISO alleviated inflammatory cell infiltration into the lung and inflammatory responses by LPS.

ISO reduces IL-1β and IL-18 production in LPS-challenged rats

IL-1β and IL-18, two inflammation-initiating cytokines, propagate injury signals and trigger inflammatory cascades in LPS-induced ALI. The levels of IL-1β and IL-18 in the BALF and lung homogenates were measured by ELISA and qPCR assay, respectively. We observed a notable reduction in the release of IL-1β (**Figure 4A**) and IL-18 (**Figure 4B**) in the BALF in LPS-treated rats with ISO post-conditioning. Similarly, enhanced mRNA expression of IL-1β (**Figure 4C**) and IL-18 (**Figure 4D**) in the lung by LPS was significantly attenuated by ISO post-treatment. These data suggest that ISO inhibited the expression and release of IL-1β and IL-18 in the lung of LPS-induced ALI rats.

ISO inhibits NLRP3 inflammasome activation in LPS-induced ALI rats

The NLRP3 inflammasome is an assembled cytosolic protein complex controlling the proteolysis activity of caspase-1, which results in the maturation of pro-IL-1β and pro-IL-18. To determine whether NLRP3 inflammasome was activated in LPS-induced ALI, mRNA and protein levels of NLRP3, ASC, and caspase-1 were assessed by qPCR and Western blot, respectively. We found that the mRNA expression of NLRP3, ASC, and caspase-1 significantly increased in the lungs of LPS-treated rats but was counteracted by ISO post-treatment (**Figure 5A-C**). The protein expression of NLRP3, ASC, and caspase-1 was consistent with their mRNA levels (**Figure 5D** and **5E**). In addition, ISO post-conditioning reduced the increase in caspase-1 activity in LPS-challenged rats (**Figure 5F**). These results indicate that the NLRP3 inflammasome was activated in LPS-induced ALI, which was attenuated by ISO post-treatment.

Inhibition of NLRP3 inflammasome activation caused by ISO depends on ROS in LPS-treated rats

ROS is involved in NLRP3 inflammasome activation in burn-induced ALI [31]. To investigate whether the inhibitory effects of ISO on NLRP3 inflammasome activation was mediated by ROS, the rats received (i.v.) NAC, the scavenger of ROS, prior to LPS injection. As shown in **Figure 6A**, ROS generation markedly increased in the lungs of LPS-challenged rats, but was reduced by ISO or NAC treatment. NAC pretreatment also reduced the expressions of NLRP3, ASC, caspase-1, and caspase-1 activity (**Figure 6B** and **6C**). The release of IL-1β (**Figure 6D**) and IL-18 (**Figure 6E**) in the BALF was decreased by NAC pretreatment. Together, these results demonstrate that ISO-exerted inhibition of NLRP3 inflammasome activation depended on ROS in the lungs of rats with LPS-induced ALI.

ISO inhibited ROS-mediated NLRP3 inflammasome activation in LPS-stimulated AMs in vitro

To partly confirm the findings in vivo, we established a cellular model of ALI using LPS-treated AMs. As shown in **Figure 7A**, ISO or NAC treatment significantly decreased LPS-induced ROS production in AMs. Increases in levels of NLRP3, ASC, and caspase-1, as well as caspase-1 activity in AMs resulting from LPS insult, were also inhibited by ISO or NAC treatment (**Figure 7B** and **7C**). Whereas the mRNA expression of IL-1β and IL-18 was enhanced by LPS stimulation, ISO or NAC treatment markedly reduced these increases (**Figure 7D** and **7E**). The release of IL-1β and IL-18 corresponded to their mRNA expression tendency (**Figure 7F** and **7G**). These results suggest that ISO attenuated LPS-induced NLRP3 inflammasome activation by

inhibiting ROS production in AMs, which is consistent with in vivo findings.

Discussion

In this study, we found that 1.4% ISO post-treatment ameliorated LPS-induced ALI by inhibiting ROS-mediated NLRP3 inflammasome activation in vivo and in vitro. The key findings were as follows. First, ISO significantly reduced the body weight loss and lung injury in LPS-challenged rats. Second, ISO abrogated LPS-induced pulmonary edema and vascular permeability. Third, ISO decreased the number of total cells, neutrophils, macrophages, and the production of IL-1β and IL-18 in the BALF of LPS-challenged rats. Fourth, ISO reduced MPO activity, the number of F4/80-positive cells, and mRNA levels of IL-1β and IL-18 in the lung tissues of LPS-treated rats. Fifth, ISO inhibited the LPS-induced formation and activation of NLRP3 inflammasome in lung tissues partly by scavenging ROS. Lastly, the pulmonary protective effects of ISO in vivo were confirmed by the in vitro studies of AMs.

LPS-induced ALI closely resembles the observed symptoms of this disorder in humans, which include damage of alveolar walls, neutrophil accumulation, and release of inflammatory cytokines [32]. Here, we found that rats with LPS injection showed significant lung injuries, as evidenced by the severe lung edema, capillary permeability, inflammatory cell infiltration, and inflammatory mediator release. In the lung, AMs are the most abundant innate immune cells and are a rich source of cytokines and chemokines that lead to neutrophil recruitment, thereby inducing further injury associated with ALI and ARDS [33-36]. In this study, we found that the numbers of total cells, neutrophils, macrophages in the BALF, MPO activity, and F4/80-positive cells in lung tissues significantly increased by LPS; these increases, however, were attenuated by ISO treatment.

IL-1β is a potent proinflammatory cytokine in both AMs initiation and the amplification of lung inflammation in patients [37]. IL-1β activates additional inflammatory cells and facilitates the release of more inflammatory mediators, which trigger inflammatory cascades and amplify injury signals [38]. IL-1β can cause alveolar edema by inducing alveolar cell surface abnormalities and alveolar epithelial and vascular endothelial permeability [7, 39]. IL-18 functions as a proinflammatory cytokine and serves as an autocrine activator that facilitates the expression of other inflammation mediators [8]. Elevated IL-18 levels are associated with morbidity and mortality in patients with ARDS [40]. Neutralization of either IL-1β or IL-18 by their antibodies has been demonstrated to prevent ALI in different rodent models [8, 13]. Our results showed that the levels of IL-1β and IL-18 in the BALF, lung tissue, and AMs increased after LPS insult. However, ISO inhibited LPS-induced mRNA expression and release of IL-1β or IL-18 in vivo and in vitro.

NLRP3 inflammasome usually responds to pathogens or endogenous danger signals during early innate immunity. NLRP3 inflammasome activation requires two steps [3]: first, microorganisms or other inflammatory factors (e.g. LPS) bind to Toll-like receptor 4 to induce the expression of NLRP3, pro-caspase-1, pro-IL-1β, and pro-IL-18 through the NF-κB pathway. And second, the extracellular ATP or bacterial toxins directly stimulate the activation of caspase-1, thereby leading to the release of IL-1β and IL-18. NLRP3 inflammasome has been shown to be activated in several models of ALI [13, 17, 41]. Activation of NLRP3 in macrophages results in increases in alveolar permeability and assembly of the NLRP3/ASC/caspase-1 complex, which facilitates caspase-1-mediated processing and release of IL-1β and IL-18 [42]. NLRP3 deletion or inhibition effectively improves hyperoxia-induced ALI [43]. In this study, we found that ISO post-treatment suppressed NLRP3 inflammasome activation caused by LPS stimulation. The inhibitory effect was evidenced by the decrease in both mRNA expression and release of IL-1β and IL-18. It was reported that ROS serves as a common signal to activate NLRP3 inflammasome [44]. Release of mitochondrial ROS can lead to subsequent NLRP3-dependent lysosomal damage and inflammasome activation [45]. Shimada et al. [46] showed that oxidized mitochondrial DNA, the ROS-oxidized product released from mitochondria, is capable of binding and activating NLRP3 inflammasome. Here, we showed that ROS production and NLRP3 inflammasome activation induced by LPS significantly decreased following ISO treatment in vivo and in vitro. Moreover, pretreatment with NAC, a broad-spectrum ROS scavenger, inhibited LPS-triggered NLRP3 inflammasome activation.

Therefore, the inhibitory effects of ISO on LPS-induced NLRP3 inflammasome signaling may partially be a ROS-dependent.

Despite these insights, our study presents several limitations. The precise mechanism by which ROS modulates NLRP3 inflammasome activation requires further investigation. Moreover, AMs were firstly activated in the pathogenesis of ALI, and then the bone-marrow derived macrophages immigrated and aggregated to the pulmonary mesenchyme to aggravate the inflammatory response. Therefore, studying the role of bone-marrow derived macrophages in LPS-induced ALI is also a worthwhile undertaking. These concepts will be the focus of our studies in the future.

In summary, ISO post-conditioning protects against LPS-induced ALI by inhibiting NLRP3 inflammasome activation, reducing IL-1β and IL-18 secretion, and restricting the inflammatory response. ROS is involved in the inhibitory effect of ISO on NLRP3 inflammasome activation. Therefore, ISO may eventually act as a potential therapeutic agent for ALI by targeting the ROS/NLRP3 signaling pathway.

Disclosure of conflict of interest

None.

Address correspondence to: Dr. Ning Yin, Department of Anesthesiology, Zhongda Hospital, School of Medicine, Southeast University, 87 Dingjiaqiao Road, Nanjing 210009, Jiangsu, China. Tel: + 86 025 83262521; Fax: + 86 025 83272011; E-mail: ningyinzhsu@sina.com

References

[1] Rubenfeld GD, Caldwell E, Peabody E, Weaver J, Martin DP, Neff M, Stern EJ and Hudson LD. Incidence and outcomes of acute lung injury. N Engl J Med 2005; 353: 1685-1693.

[2] Matthay MA, Ware LB and Zimmerman GA. The acute respiratory distress syndrome. J Clin Invest 2012; 122: 2731-2740.

[3] Gross O, Thomas CJ, Guarda G and Tschopp J. The inflammasome: an integrated view. Immunol Rev 2011; 243: 136-151.

[4] Strowig T, Henao-Mejia J, Elinav E and Flavell R. Inflammasomes in health and disease. Nature 2012; 481: 278-286.

[5] Franchi L, Munoz-Planillo R and Nunez G. Sensing and reacting to microbes through the inflammasomes. Nat Immunol 2012; 13: 325-332.

[6] Zhou R, Tardivel A, Thorens B, Choi I and Tschopp J. Thioredoxin-interacting protein links oxidative stress to inflammasome activation. Nat Immunol 2010; 11: 136-140.

[7] Ganter MT, Roux J, Miyazawa B, Howard M, Frank JA, Su G, Sheppard D, Violette SM, Weinreb PH, Horan GS, Matthay MA and Pittet JF. Interleukin-1beta causes acute lung injury via alphavbeta5 and alphavbeta6 integrin-dependent mechanisms. Circ Res 2008; 102: 804-812.

[8] Jordan JA, Guo RF, Yun EC, Sarma V, Warner RL, Crouch LD, Senaldi G, Ulich TR and Ward PA. Role of IL-18 in acute lung inflammation. J Immunol 2001; 167: 7060-7068.

[9] Mao K, Chen S, Chen M, Ma Y, Wang Y, Huang B, He Z, Zeng Y, Hu Y, Sun S, Li J, Wu X, Wang X, Strober W, Chen C, Meng G and Sun B. Nitric oxide suppresses NLRP3 inflammasome activation and protects against LPS-induced septic shock. Cell Res 2013; 23: 201-212.

[10] Dolinay T, Kim YS, Howrylak J, Hunninghake GM, An CH, Fredenburgh L, Massaro AF, Rogers A, Gazourian L, Nakahira K, Haspel JA, Landazury R, Eppanapally S, Christie JD, Meyer NJ, Ware LB, Christiani DC, Ryter SW, Baron RM and Choi AM. Inflammasome-regulated cytokines are critical mediators of acute lung injury. Am J Respir Crit Care Med 2012; 185: 1225-1234.

[11] Xu P, Wen Z, Shi X, Li Y, Fan L, Xiang M, Li A, Scott MJ, Xiao G, Li S, Billiar TR, Wilson MA and Fan J. Hemorrhagic shock augments Nlrp3 inflammasome activation in the lung through impaired pyrin induction. J Immunol 2013; 190: 5247-5255.

[12] Niesler U, Palmer A, Radermacher P and Huber-Lang MS. Role of alveolar macrophages in the inflammatory response after trauma. Shock 2014; 42: 3-10.

[13] Wu J, Yan Z, Schwartz DE, Yu J, Malik AB and Hu G. Activation of NLRP3 inflammasome in alveolar macrophages contributes to mechanical stretch-induced lung inflammation and injury. J Immunol 2013; 190: 3590-3599.

[14] Jacobs RF, Tabor DR, Burks AW and Campbell GD. Elevated interleukin-1 release by human alveolar macrophages during the adult respiratory distress syndrome. Am Rev Respir Dis 1989; 140: 1686-1692.

[15] Eyal FG, Hamm CR and Parker JC. Reduction in alveolar macrophages attenuates acute ventilator induced lung injury in rats. Intensive Care Med 2007; 33: 1212-1218.

[16] Lindauer ML, Wong J, Iwakura Y and Magun BE. Pulmonary inflammation triggered by ricin toxin requires macrophages and IL-1 signaling. J Immunol 2009; 183: 1419-1426.

[17] Jones HD, Crother TR, Gonzalez-Villalobos RA, Jupelli M, Chen S, Dagvadorj J, Arditi M and Shimada K. The NLRP3 inflammasome is re-

quired for the development of hypoxemia in LPS/mechanical ventilation acute lung injury. Am J Respir Cell Mol Biol 2014; 50: 270-280.
[18] Statler KD, Alexander H, Vagni V, Holubkov R, Dixon CE, Clark RS, Jenkins L and Kochanek PM. Isoflurane exerts neuroprotective actions at or near the time of severe traumatic brain injury. Brain Res 2006; 1076: 216-224.
[19] Tsutsumi YM, Patel HH, Lai NC, Takahashi T, Head BP and Roth DM. Isoflurane produces sustained cardiac protection after ischemia-reperfusion injury in mice. Anesthesiology 2006; 104: 495-502.
[20] Lee HT, Emala CW, Joo JD and Kim M. Isoflurane improves survival and protects against renal and hepatic injury in murine septic peritonitis. Shock 2007; 27: 373-379.
[21] Li JT, Wang H, Li W, Wang LF, Hou LC, Mu JL, Liu X, Chen HJ, Xie KL, Li NL and Gao CF. Anesthetic isoflurane posttreatment attenuates experimental lung injury by inhibiting inflammation and apoptosis. Mediators Inflamm 2013; 2013: 108928.
[22] Mu J, Xie K, Hou L, Peng D, Shang L, Ji G, Li J, Lu Y and Xiong L. Subanesthetic dose of isoflurane protects against zymosan-induced generalized inflammation and its associated acute lung injury in mice. Shock 2010; 34: 183-189.
[23] Li QF, Zhu YS, Jiang H, Xu H and Sun Y. Isoflurane preconditioning ameliorates endotoxin-induced acute lung injury and mortality in rats. Anesth Analg 2009; 109: 1591-1597.
[24] Fujinaga T, Nakamura T, Fukuse T, Chen F, Zhang J, Ueda S, Hamakawa H, Omasa M, Sakai H, Hanaoka N, Wada H and Bando T. Isoflurane inhalation after circulatory arrest protects against warm ischemia reperfusion injury of the lungs. Transplantation 2006; 82: 1168-1174.
[25] Plachinta RV, Hayes JK, Cerilli LA and Rich GF. Isoflurane pretreatment inhibits lipopolysaccharide-induced inflammation in rats. Anesthesiology 2003; 98: 89-95.
[26] Reutershan J, Chang D, Hayes JK and Ley K. Protective effects of isoflurane pretreatment in endotoxin-induced lung injury. Anesthesiology 2006; 104: 511-517.
[27] Flondor M, Hofstetter C, Boost KA, Betz C, Homann M and Zwissler B. Isoflurane inhalation after induction of endotoxemia in rats attenuates the systemic cytokine response. Eur Surg Res 2008; 40: 1-6.
[28] Dong X, Hu R, Sun Y, Li Q and Jiang H. Isoflurane post-treatment improves pulmonary vascular permeability via upregulation of heme oxygenase-1. Exp Lung Res 2013; 39: 295-303.
[29] Lavnikova N, Prokhorova S, Helyar L and Laskin DL. Isolation and partial characterization of subpopulations of alveolar macrophages, granulocytes, and highly enriched interstitial macrophages from rat lung. Am J Respir Cell Mol Biol 1993; 8: 384-392.
[30] Wang S, Zhao J, Wang H, Liang Y, Yang N and Huang Y. Blockage of P2X7 attenuates acute lung injury in mice by inhibiting NLRP3 inflammasome. Int Immunopharmacol 2015; 27: 38-45.
[31] Han S, Cai W, Yang X, Jia Y, Zheng Z, Wang H, Li J, Li Y, Gao J, Fan L and Hu D. ROS-Mediated NLRP3 Inflammasome Activity Is Essential for Burn-Induced Acute Lung Injury. Mediators Inflamm 2015; 2015: 720457.
[32] Chen H, Bai C and Wang X. The value of the lipopolysaccharide-induced acute lung injury model in respiratory medicine. Expert Rev Respir Med 2010; 4: 773-783.
[33] Monton C and Torres A. Lung inflammatory response in pneumonia. Monaldi Arch Chest Dis 1998; 53: 56-63.
[34] Beck-Schimmer B, Schwendener R, Pasch T, Reyes L, Booy C and Schimmer RC. Alveolar macrophages regulate neutrophil recruitment in endotoxin-induced lung injury. Respir Res 2005; 6: 61.
[35] Lomas-Neira J, Chung CS, Perl M, Gregory S, Biffl W and Ayala A. Role of alveolar macrophage and migrating neutrophils in hemorrhage-induced priming for ALI subsequent to septic challenge. Am J Physiol Lung Cell Mol Physiol 2006; 290: L51-58.
[36] Puneet P, Moochhala S and Bhatia M. Chemokines in acute respiratory distress syndrome. Am J Physiol Lung Cell Mol Physiol 2005; 288: L3-15.
[37] Dinarello CA. Biologic basis for interleukin-1 in disease. Blood 1996; 87: 2095-2147.
[38] Goodman RB, Pugin J, Lee JS and Matthay MA. Cytokine-mediated inflammation in acute lung injury. Cytokine Growth Factor Rev 2003; 14: 523-535.
[39] Hybertson BM, Lee YM, Cho HG, Cho OJ and Repine JE. Alveolar type II cell abnormalities and peroxide formation in lungs of rats given IL-1 intratracheally. Inflammation 2000; 24: 289-303.
[40] Makabe H, Kojika M, Takahashi G, Matsumoto N, Shibata S, Suzuki Y, Inoue Y and Endo S. Interleukin-18 levels reflect the long-term prognosis of acute lung injury and acute respiratory distress syndrome. J Anesth 2012; 26: 658-663.
[41] Grailer JJ, Canning BA, Kalbitz M, Haggadone MD, Dhond RM, Andjelkovic AV, Zetoune FS and Ward PA. Critical role for the NLRP3 inflammasome during acute lung injury. J Immunol 2014; 192: 5974-5983.
[42] Kolliputi N, Galam L, Parthasarathy PT, Tipparaju SM and Lockey RF. NALP-3 inflammasome silencing attenuates ceramide-induced tran-

sepithelial permeability. J Cell Physiol 2012; 227: 3310-3316.
[43] Fukumoto J, Fukumoto I, Parthasarathy PT, Cox R, Huynh B, Ramanathan GK, Venugopal RB, Allen-Gipson DS, Lockey RF and Kolliputi N. NLRP3 deletion protects from hyperoxia-induced acute lung injury. Am J Physiol Cell Physiol 2013; 305: C182-189.
[44] Dostert C, Petrilli V, Van Bruggen R, Steele C, Mossman BT and Tschopp J. Innate immune activation through Nalp3 inflammasome sensing of asbestos and silica. Science 2008; 320: 674-677.
[45] Heid ME, Keyel PA, Kamga C, Shiva S, Watkins SC and Salter RD. Mitochondrial reactive oxygen species induces NLRP3-dependent lysosomal damage and inflammasome activation. J Immunol 2013; 191: 5230-5238.
[46] Shimada K, Crother TR, Karlin J, Dagvadorj J, Chiba N, Chen S, Ramanujan VK, Wolf AJ, Vergnes L, Ojcius DM, Rentsendorj A, Vargas M, Guerrero C, Wang Y, Fitzgerald KA, Underhill DM, Town T and Arditi M. Oxidized mitochondrial DNA activates the NLRP3 inflammasome during apoptosis. Immunity 2012; 36: 401-414.